

Anomalous Magnetic Field Effects on Photochemical Reactions in Ionic Liquid under Ultrahigh Fields of up to 28 T

Atom Hamasaki,[†] Tomoaki Yago,[†] Tadashi Takamasu,[‡] Giyuu Kido,[‡] and Masanobu Wakasa^{*,†}

Department of Chemistry, Graduate School of Science and Engineering, Saitama University, 255 Shimo-okubo, Sakura-ku, Saitama-shi, Saitama 338-8570, Japan, and National Institute for Materials Science (NIMS), 3-13 Sakura, Tsukuba, Ibaraki 305-0003, Japan

Received: October 16, 2007; In Final Form: December 21, 2007

The magnetic field effects (MFEs) on photoinduced hydrogen abstraction reactions between benzophenone and thiophenol in an ionic liquid, *N,N,N*-trimethyl-*N*-propylammonium bis(trifluoromethanesulfonyl) imide (TMPA TFSI), were studied by a nanosecond laser flash photolysis technique under ultrahigh fields of up to 28 T. Extremely large and anomalous stepwise MFEs were observed for the first time. The escape yield of benzophenone ketyl radical decreased with increasing magnetic field strength (B) at $0 \text{ T} < B \leq 2 \text{ T}$. The decrease was almost saturated at $2 \text{ T} < B \leq 10 \text{ T}$. At much higher fields ($10 \text{ T} < B \leq 28 \text{ T}$), the yield decreased again with increasing B , producing a 25% decrease at 28 T.

Introduction

Magnetic field effects (MFEs) on photochemical reactions through radical pairs and biradicals have received considerable attention during the past three decades. Magnetic fields interact with the electron spins of radical pairs, and thus the spin conversion of the radical pairs between singlet (S) and triplet (T_m , $m = 0, \pm 1$) states is influenced by the fields. The lifetime of the radical pairs and the yield of the escaped radicals consequently show appreciable MFEs. A large number of interesting phenomena on spin dynamics have already been reported.^{1,2} On the other hand, ionic liquids (ILs), which are considered as one of the most promising new solvents in green chemistry, have gained much attention because of their unusual chemical properties: nonvolatile, noncorrosive, nonflammable, stable in air and moisture, and designable.^{3–8} Some results observed in ILs are, however, quite different from those observed in conventional solvents.^{9–13} Hamaguchi et al. reported that the photoisomerization indeed proceeds in 1-butyl-3-methylimidazolium hexafluorophosphate ([bmim]PF₆) with a rate much larger than that expected from its polarity and viscosity.⁹ McLean et al. reported the hydrogen abstraction reactions from ILs by benzophenone (BP) and the photoelectron transfer from ruthenium (II) tris(bipyridyl) to methylviologen in [bmim]PF₆.^{10,11} García et al. reported that a series of photochemical reactions covering energy transfer, hydrogen transfer, and electron transfer was studied in [bmim]PF₆.¹² Recently, we found extremely large MFEs in ILs; the escape yield of benzophenone ketyl radical generated from the photoinduced hydrogen abstraction reaction of BP with thiophenol (PhSH) in *N,N,N*-trimethyl-*N*-propylammonium bis(trifluoromethanesulfonyl) imide (TMPA TFSI) decreased by 20% at 1.7 T.¹³ The observed MFEs could not be explained by the high viscosity of the IL alone, but a local structure in the IL was

suggested as an origin of the large MFEs. To clarify the local structure of ILs and to find a new classified MFE, the complete MFEs data set from 0 T up to 28 T in ILs is necessary. Therefore, using a pulsed magnet, we studied the MFEs on the photoinduced hydrogen abstraction reaction of BP with PhSH in TMPA TFSI under ultrahigh magnetic fields of up to 28 T.

Experimental

Materials. TMPA TFSI (Cica) was used as received. PhSH (Cica) was purified by vacuum distillation. BP (Cica) was recrystallized from methanol. The concentrations of BP and PhSH in the employed ILs were 2.0×10^{-2} and 1.2×10^{-1} mol dm⁻³, respectively. The viscosity and density of TMPA TFSI were measured by a Yamauchi VM-10A-L viscometer and an Anton Paar DMA 5000 density meter.

Nanosecond Laser Flash Photolysis. Laser flash photolysis experiments were carried out at 296 K using an apparatus described elsewhere.^{14,15} The third harmonic (355 nm) of a Quanta-Ray GCR-130-10 nanosecond Nd:YAG laser was used as an excitation light source. A double-beam probe system was used for measuring the transient absorption accurately. The transient absorption was recorded by a Hewlett-Packard HP54522A digitizing oscilloscope (2 GHz) with a Hamamatsu R636 photomultiplier. The argon-bubbled solution in a quartz cell was placed at the center of a pulsed magnet. The pulsed magnet had a room-temperature bore with a diameter of 20 mm and a length of 160 mm. Pulsed magnetic fields were generated by supplying intense pulsed currents from a 10 mF capacitor bank of 125 kJ at 5 kV. The maximum field was 32.2 T at 3.5 kV. Applied magnetic field was measured with a search coil placed right next to the quartz cell.

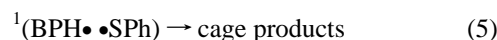
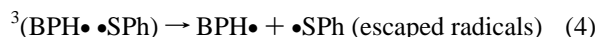
Results and Discussion

The reaction scheme of photoinduced hydrogen abstraction reaction between BP and PhSH can be represented as follows:

* To whom correspondence should be addressed. E-mail: mwakasa@chem.saitama-u.ac.jp.

[†] Saitama University.

[‡] National Institute for Materials Science (NIMS).



Here, ${}^1\text{BP}^*$, ${}^3\text{BP}^*$, $\text{BPH}\bullet$, and $\bullet\text{SPh}$ represent the singlet and triplet excited states of benzophenone, benzophenone ketyl, and phenylthiyl radicals, respectively. ${}^1(\text{BPH}\bullet \bullet \text{SPh})$ and ${}^3(\text{BPH}\bullet \bullet \text{SPh})$ denote singlet and triplet radical pairs composed of benzophenone ketyl and phenylthiyl radicals, respectively. This reaction system showed appreciable MFEs, even in nonviscous homogeneous solutions such as methanol ($\eta = 0.55$ cP) and ethanol ($\eta = 1.08$ cP).¹⁶ Thus the rate constant of the recombination can safely be estimated to be as large as 10^9 – 10^{10} s^{-1} because no MFE should be observed when the recombination reaction (eq 5) is much slower than the escaping process ($>10^9$ s^{-1}) (eq 4).

Since $\text{BPH}\bullet$ has transient absorption bands around 380 and 550 nm,¹⁷ the magnetic field dependence of the time profile of the transient absorption, $A(t)$, was measured at 380 nm. At 0 T $< B \leq 0.05$ T, no change of the $A(t)$ curve was observed within the experimental error, but at above 0.1 T, it showed clear MFEs. Figure 1 typically shows the $A(t)$ curves observed at 0 and 28 T. The decay of each $A(t)$ curve has fast and slow decay components. The fast component is ascribable to the decay of radical pairs, and the slow one can be ascribed to the escaped $\text{BPH}\bullet$. As shown in Figure 1, the first decay component due to the radical pairs is clearly affected by the fields. Since the lifetime of triplet–triplet absorption (${}^3\text{BP}^*$) observed at 520 nm was 85 ns, the $A(0.75 \mu\text{s})$ value is proportional to the escaped radical yield ($Y(B)$). Thus, the ratio $R(B) = Y(B)/Y(0 \text{ T}) = A(0.75 \mu\text{s}, B \text{ T})/A(0.75 \mu\text{s}, 0 \text{ T})$ gives the MFE on the yield of the escaped $\text{BPH}\bullet$. In the present study, $R(28 \text{ T})$ was obtained to be 0.75 ± 0.02 . This means that the yield of the escaped $\text{BPH}\bullet$ decreased by 25% at 28 T compared with that at 0 T.

Next, the $R(B)$ values are plotted against B in Figure 2. The stepwise field dependence of $R(B)$ can be summarized as follows: (1) $R(B)$ decreased with increasing B at 0 T $< B \leq 2$ T. (2) The decrease was almost saturated at 2 T $< B \leq 10$ T, producing $R(10 \text{ T})$ of 0.79. (3) At much higher fields (10 T $< B \leq 28$ T), $R(B)$ decreased again with increasing B . In Figure 3, the reaction scheme, triplet–singlet (T–S) spin conversion, and spin relaxation of the present radical pairs at (a) $B = 0$ T, (b) 0 T $< B \leq 2$ T, (c) 2 T $< B \leq 10$ T, and (d) 10 T $< B \leq 28$ T are schematically shown. Here S and T denote singlet and triplet radical pairs, respectively. Y represents the yield of the process described in the figure. k_{esc} , k_{HFCM} , $k_{\Delta\text{gM}}$, and k_{SR} are the rate constants of the escaping process, T–S spin conversion due to the hyperfine coupling mechanism (HFCM) and the Δg mechanism (ΔgM), and spin relaxation, respectively.

The decrease of $R(B)$ at 0 T $< B \leq 2$ T and the saturation of MFEs at 2 T $< B \leq 10$ T can safely be explained by the ΔgM , which originates from the difference between the isotropic g factors of two radicals in a pair,^{1,2,16,18} because the present radical pair of $\text{BPH}\bullet$ ($g = 2.0030$) and $\bullet\text{SPh}$ ($g = 2.0082$) has a large Δg value of 0.0052.¹⁸ Moreover, the plots of $R(B)$ vs $B^{1/2}$ have a good linear relationship, as shown in Figure 2 (inset). Such field dependence of the linear relationship is well-known to the MFEs due to the ΔgM .¹⁶

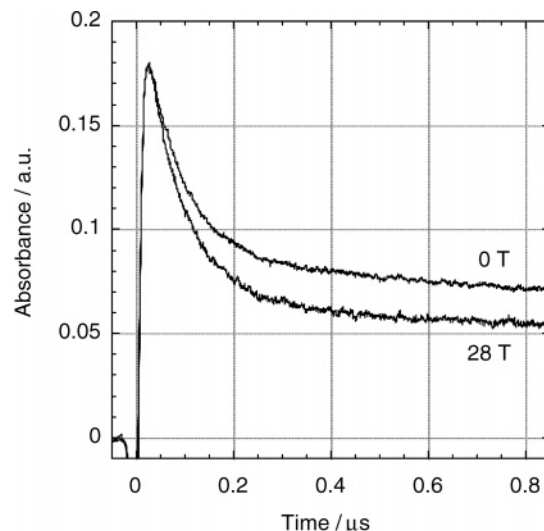


Figure 1. $A(t)$ curves observed at 380 nm for the photoinduced hydrogen abstraction reaction of BP with PhSH in TMPA TFSI at 0 and 28 T.

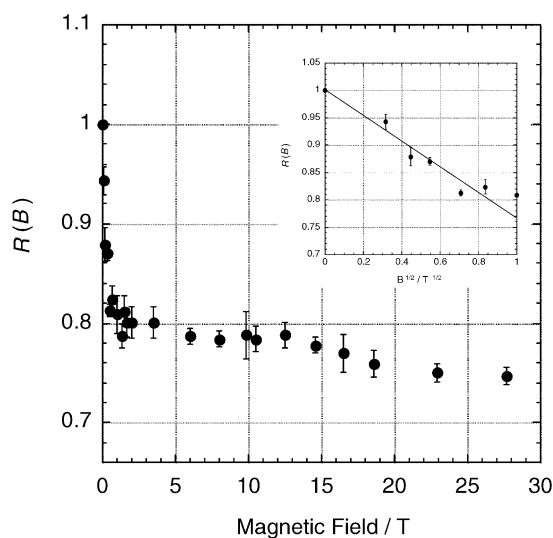


Figure 2. Magnetic field dependence of the yield of escaped $\text{BPH}\bullet$ ($R(B) = A(0.75 \mu\text{s}, B \text{ T})/A(0.75 \mu\text{s}, 0 \text{ T})$) observed at 380 nm in TMPA TFSI. Inset: Plots of $R(B)$ against $B^{1/2}$ at 0 T $\leq B \leq 1$ T.

The saturation of MFEs due to the ΔgM has previously been reported for the similar reaction of 4-methoxybenzophenone with PhSH in nonviscous conventional solvents such as 2-methyl-1-propanol.¹⁸ In 2-methyl-1-propanol ($\eta < 3.3$ cP), the escaping process from the radical pairs is much faster than the T–S spin conversion process. At 0 T, almost all of triplet radical pairs are escaped from the pairs. In the high field region, the spin conversion of T_0 –S is accelerated by the ΔgM , and it becomes much faster than the escaping process. As the limiting value of the yield of the T_0 –S spin conversion process, 33% of the triplet radical pairs (T_0) can convert to the singlet pairs and disappear by the recombination process. Therefore, the saturation of $R(B)$ was observed in the high field region, producing an $R(B)$ of 0.66. In the present study, however, $R(B)$ observed at the saturated field was as large as 0.79. Such large $R(B)$ values can be explained by the escaping rate of the triplet pairs in TMPA TFSI. Since the viscosity of TMPA TFSI (72.6 cP) is much larger than that of 2-methyl-1-propanol (3.3 cP), the escaping process of the triplet pairs in TMPA TFSI should be slow. Thus a part of the triplet pairs can convert to the singlet pairs, even at 0 T, and disappear by the recombination process, as shown

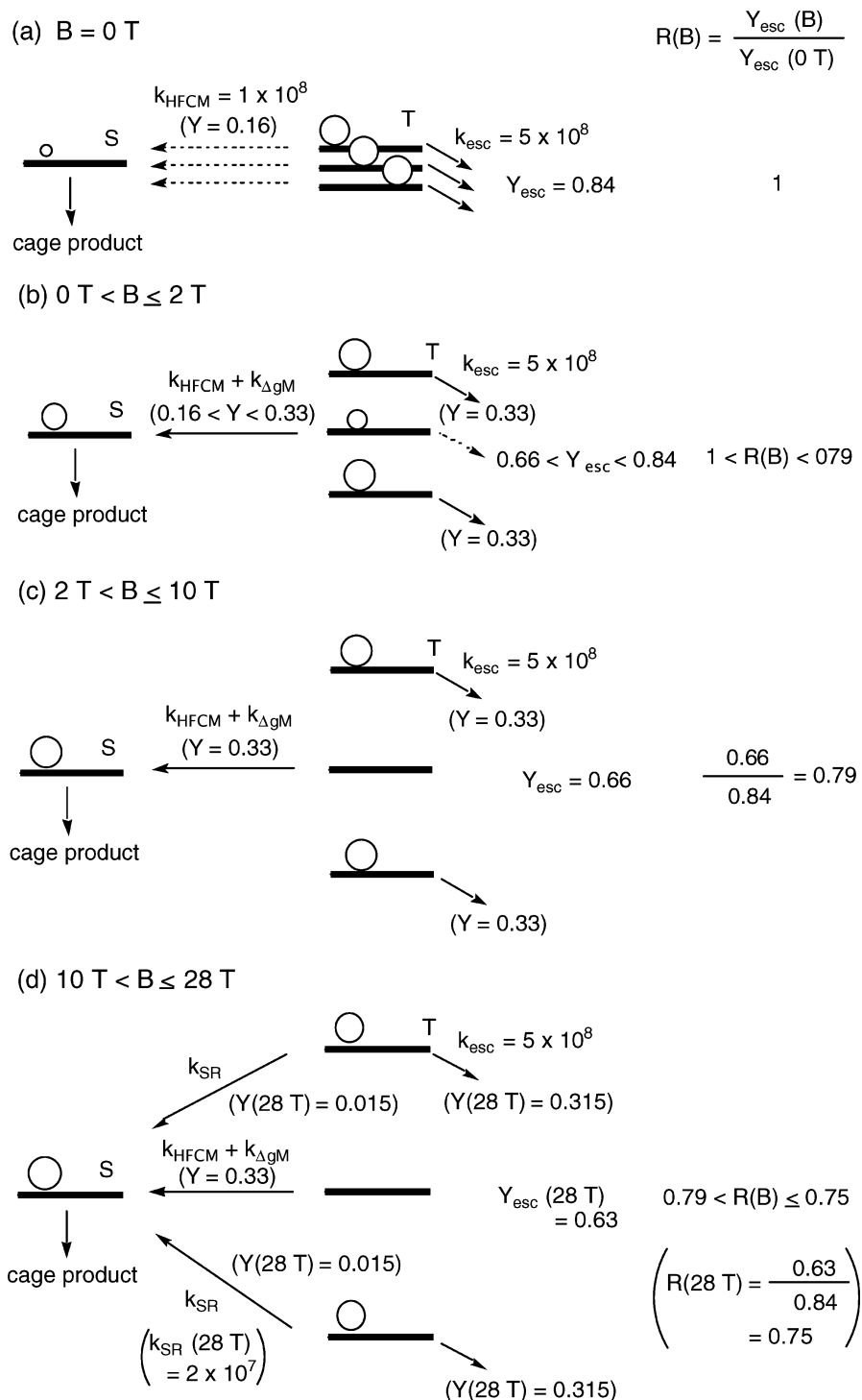


Figure 3. Reaction scheme, T–S spin conversion and spin relaxation of the present radical pairs generated from a triplet precursor at (a) $B = 0 \text{ T}$, (b) $0 \text{ T} < B \leq 2 \text{ T}$, (c) $2 \text{ T} < B \leq 10 \text{ T}$, and (d) $10 \text{ T} < B \leq 28 \text{ T}$.

in Figure 3(a). The escaped radical (Y_{esc}) at 0 T in TMPA TFSI was estimated to be 0.84, which was discussed later. With increasing B at $0 \text{ T} < B \leq 2 \text{ T}$, as shown in Figure 3(b), the spin conversion of T_0 –S is accelerated by the ΔgM , thus Y_{esc} decreases from 0.84. At the saturated fields of $2 \text{ T} < B \leq 10 \text{ T}$, the rate constant of T_0 –S spin conversion due to the ΔgM ($k_{\Delta gM}$) is much larger than the rate constant of the escaping process: $k_{\Delta gM}$ at 10 T was calculated to be $2.3 \times 10^9 \text{ s}^{-1}$ from the Δg value of 0.0052. Thus almost all of triplet radical pairs in the T_0 state (33%) can convert to singlet pairs and disappear by the recombination process. As clearly seen in Figure 3(c), Y_{esc} became 0.66, resulting in the $R(B)$ ($= Y_{\text{esc}}(B)/Y_{\text{esc}}(0 \text{ T})$) of

0.79. Using these values, we can estimate that 16% of the triplet radical pairs at 0 T convert to singlet radical pairs and disappear by the recombination process. This means that Y_{esc} is 0.84. Since k_{HFCM} can roughly be estimated to be $1 \times 10^8 \text{ s}^{-1}$ from the HFC constants of BPH• and PhS•, k_{esc} is calculated to be $5 \times 10^8 \text{ s}^{-1}$ using the simple kinetic model as shown in Figure 3(a).

In a previous paper,¹⁸ the $R(B)$ values in 2-methyl-1-propanol were saturated above 20 T, and the observed $R(B)$ values could be reproduced fairly well by the diffusion model. According to the diffusion model developed for the MFE in such conventional solvents, the saturated fields due to the ΔgM should decrease with increasing the solvent viscosity.^{19,20} Thus we tried to

estimate the viscosity needed for the saturation of the MFEs at 2 T using the diffusion model together with the Δg M. However, the estimated viscosity of 400 cP is much larger than that of TMPA TFSI (72.6 cP). Therefore the saturation of the MFEs at 2 T cannot be explained by the viscosity of the IL alone. The cage effect of ILs is the most likely candidate to explain the observed saturation. If ILs have the local structure like a micellar solution, it can work as a cage for the photochemical reactions and cause the saturation of the MFEs at the low field region. In fact, the local structure or some domains in ILs were recently reported by Hamaguchi et al.,²¹ Wang et al.,²² Nishikawa et al.,²³ and Wishart et al.²⁴

The secondary decrease of $R(B)$ at $10 \text{ T} < B \leq 28 \text{ T}$ may be due to the relaxation mechanism (RM), which originates from the spin relaxation of $T_{\pm 1}-T_0$ and $T_{\pm 1}-S$. According to the RM by Hayashi and Nagakura,²⁵ the spin relaxation rates of k_R and $k_{R'}$ for a radical pair consisting of radical A and radical B can be represented as follows:^{1,2,25}

$$k_R = k_{dd} + k_A + k_B \quad (6)$$

$$k_{R'} = k_A + k_B \quad (7)$$

Here, k_R is the spin relaxation rate between $T_{\pm 1}$ and T_0 , and $k_{R'}$ is that between $T_{\pm 1}$ and S . k_{dd} is the rate constant for the inter-radical relaxation induced by the electron spin–spin interaction. k_j ($j = A, B$) is the rate constant for the intra-radical relaxation of radical j . k_j can be given by

$$k_j = k_j^{\delta\text{HFC}} + k_j^{\delta g} \quad (8)$$

Here, $k_j^{\delta\text{HFC}}$ and $k_j^{\delta g}$ are the rate constants of spin–lattice relaxation by the anisotropic hyperfine coupling and the anisotropic Zeeman interaction, respectively. The magnetic field dependence of k_R and $k_{R'}$ can be calculated from the analytical forms of k_{dd} , $k_j^{\delta\text{HFC}}$, and $k_j^{\delta g}$ as follows:

$$k_{dd} = \frac{\mu_B^4 g_A^2 g_B^2}{10\hbar^2 R^6} \frac{3\tau_{AB}}{1 + \omega^2 \tau_{AB}^2} \quad (9)$$

$$k_j^{\delta\text{HFC}} = \frac{1}{30\hbar^2} \delta a_j^2 \frac{2\tau_j}{1 + \omega^2 \tau_j^2} \quad (10)$$

$$k_j^{\delta g} = \frac{1}{30\hbar^2} \mu_B^2 B^2 \delta g_j^2 \frac{2\tau_j}{1 + \omega^2 \tau_j^2} \quad (11)$$

$$\omega = \hbar^{-1} g \mu_B B \quad (12)$$

Here g_A and g_B represent the isotropic g values of radicals A and B, respectively. τ_{AB} is the correlation time of the radical pair. δa and δg denote the difference of the anisotropic hyperfine coupling constants ($|A_{\parallel} - A_{\perp}|$) and the difference of the anisotropic g values ($|g_{\parallel} - g_{\perp}|$), respectively. τ_j is the correlation time of each component radical. We can see from eqs 9–12 that k_{dd} and $k_j^{\delta\text{HFC}}$ decrease with increasing B , but $k_j^{\delta g}$ increases with increasing B . The $k_R + k_{R'}$ values were calculated with the following parameters (subscripts denote the individual radicals; A for BPH• and B for PhS•): $g_A = 2.0030$,¹⁸ $g_B = 2.0082$,¹⁸ $\delta a_A/g\mu_B = 0.002 \text{ T}$,^{26,27} $\delta a_B/g\mu_B = 0.002 \text{ T}$,^{15,28} $\delta g_A = 0.002$,^{26,27} $\delta g_B = 0.02$,^{15,28} $\tau_A = \tau_B = 1.0 \times 10^{-12} \text{ s}$,^{15,26,27} $\tau_{AB} = 1.0 \times 10^{-10} \text{ s}$,^{15,28} and $R = 1.0 \text{ nm}$.^{15,27} Here the correlation time (τ_j) of $1 \times 10^{-12} \text{ s}$ is much smaller than that estimated from the viscosity of TMPA TFSI ($\eta = 72.6 \text{ cP}$).

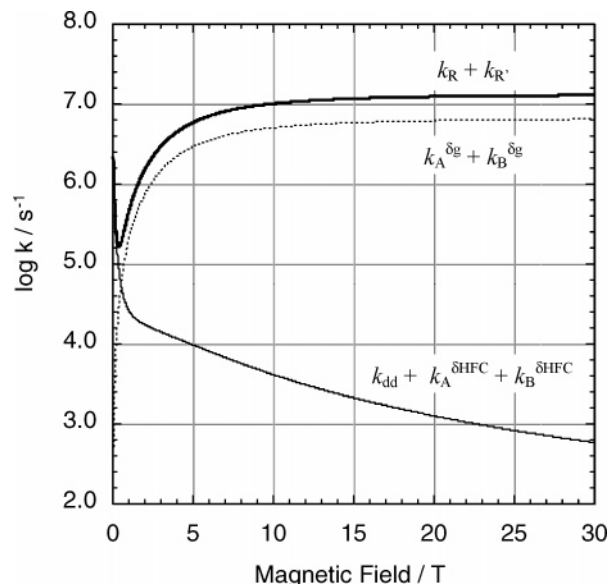


Figure 4. Calculated magnetic field dependence of the spin relaxation rates of $k_R + k_{R'}$, $k_{dd} + k_A^{\delta\text{HFC}} + k_B^{\delta\text{HFC}}$, and $k_A^{\delta g} + k_B^{\delta g}$ for a model radical pair having the following parameters (subscripts denote the individual radicals; radical A for BPH• and radical B for PhS•): $g_A = 2.0030$, $g_B = 2.0082$, $\delta a_A/g\mu_B = 0.002 \text{ T}$, $\delta a_B/g\mu_B = 0.002 \text{ T}$, $\delta g_A = 0.002$, $\delta g_B = 0.02$, $\tau_A = \tau_B = 1.0 \times 10^{-12} \text{ s}$, $\tau_{AB} = 1.0 \times 10^{-10} \text{ s}$, and $R = 1.0 \text{ nm}$.

Since local structure or some domains in the ILs were suggested, the microscopic viscosity in such structure or domains may be small, resulting in a small correlation time. In the previous paper, no MFE was observed in a viscous homogeneous solvent (cyclohexanol/2-methyl-1-propanol (100:1(v/v)), $\eta = 54.8 \text{ cP}$) using the same reaction system.¹³ If the microscopic viscosity in TMPA TFSI is similar to the bulk viscosity (72.6 cP), the MFEs should not be observed. Thus the microscopic viscosity in the IL is considered to be very small. Similar results were reported by Hamaguchi et al.⁹ In their paper, photoisomerization of *trans*-stilbene in an IL occurred efficiently in spite of its large viscosity. This may be due to the small microscopic viscosity of the IL. In Figure 4, $\log(k_R + k_{R'})$, $\log(k_{dd} + k_A^{\delta\text{HFC}} + k_B^{\delta\text{HFC}})$, and $\log(k_A^{\delta g} + k_B^{\delta g})$ values are plotted against B . The calculated $k_R + k_{R'}$ values show clear B dependence as follows: (1) At the low field region, $k_R + k_{R'}$ decreases with increasing B . (2) At the high field region, $k_R + k_{R'}$ increases gradually with increasing B . (3) At 28 T, $k_R + k_{R'}$ is estimated to be $1.2 \times 10^7 \text{ s}^{-1}$. As seen in Figure 4, the spin relaxation of $T_{\pm 1}-T_0$ and $T_{\pm 1}-S$ can compete with the escaping process only at the high field region. The spin relaxation causes the decrease of Y_{esc} . The MFEs observed at $10 \text{ T} < B \leq 28 \text{ T}$ can be explained by this mechanism (RM) and rationalized by Figure 3(d). Using the simple kinetic model as shown in Figure 3(d) and the observed R (28 T) value of 0.75, k_{SL} at 28 T is estimated to be $2 \times 10^7 \text{ s}^{-1}$. This k_{SL} value agrees well with the calculated $k_R + k_{R'}$ value of $1.2 \times 10^7 \text{ s}^{-1}$. Therefore, the MFEs observed in the present study at $10 \text{ T} < B \leq 28 \text{ T}$ can be explained by the RM with the small correlation time.

The alternative mechanism for the observed sequential increase in the MFEs is an anisotropic Δg -induced $S-T_0$ intersystem crossing transitions in rotation-hindered radical pairs. If rotation is slow enough, different pairs will experience different local Δg . The rotation-hindered radical pairs with small Δg might have insufficiently rapid intersystem crossing in a given field but it can be accelerated at higher fields. Since such local Δg values could not be obtained directly from the

experiments, more theoretical studies using the stochastic Liouville equation are now in progress, but these are beyond the scope of the present experimental paper.

Conclusions

MFEs on the photoinduced hydrogen abstract reactions of BP with PhSH in TPA TFSI were investigated under ultrahigh fields of up to 28 T. Large and anomalous stepwise MFEs were observed. The MFEs observed at $0 \text{ T} < B \leq 2 \text{ T}$ and the saturation of MFEs at $2 \text{ T} < B \leq 10 \text{ T}$ can be explained by the ΔgM , and those observed at $10 \text{ T} < B \leq 28 \text{ T}$ can be explained by the RM. Using the simple kinetic model and the observed R (28 T) value, the spin relaxation rate (k_{SL}) at 28 T is experimentally estimated to be $2 \times 10^7 \text{ s}^{-1}$ and is rationalized by the theoretically calculated $k_R + k_R'$ value of $1.2 \times 10^7 \text{ s}^{-1}$. The MFEs due to the RM cannot be observed in conventional solvents, but can in micellar solutions. Therefore, it is noteworthy that the large cage effect of the IL plays an important role in the secondary decrease of $R(B)$.

Acknowledgment. This work was partially supported by a Grant-in-Aid for Scientific Research (No. 17073002) in Priority Area "Science of Ionic Liquids" (Area Number 452) from the Ministry of Education, Culture, Sports, Science, and Technology of Japan.

References and Notes

- (1) Steiner, U. E.; Ulrich, T. *Chem. Rev.* **1989**, *89*, 51.
- (2) Nagakura, S.; Hayashi, H.; Azumi, T. *Dynamic Spin Chemistry*; Kodansha-Wiley: Tokyo, New York, 1998.
- (3) Seddon, K. R. *J. Chem. Technol. Biotechnol.* **1997**, *68*, 351.
- (4) Welton, T. *Chem. Rev.* **1999**, *99*, 2071.

- (5) Wasserscheid, P.; Keim, W. *Angew. Chem., Int. Ed.* **2000**, *39*, 3772.
- (6) Sheldon, R. *Chem. Commun.* **2001**, 2399.
- (7) Dupont, J.; Souza, R. F.; Saurez, P. A. Z. *Chem. Rev.* **2002**, *102*, 3667.
- (8) Ohno, H. *Electrochemical Aspects of Ionic Liquids*; John Wiley & Sons, Inc.: Hoboken, NJ, 2005.
- (9) Ozawa, R.; Hamaguchi, H. *Chem. Lett.* **2001**, *30*, 736.
- (10) Muldoon, M. J.; McLean, A. J.; Gordon, C. M.; Dunkin, I. R. *Chem. Commun.* **2001**, 2364.
- (11) Gordon, C. M.; McLean, A. J. *Chem. Commun.* **2000**, 1395.
- (12) Álvaro, M.; Ferrer, B.; Gracia, H.; Narayana, M. *Chem. Phys. Lett.* **2002**, *362*, 435.
- (13) Wakasa, M. *J. Phys. Chem. B* **2007**, *111*, 9434.
- (14) Hamasaki, A.; Nishizawa, K.; Sakaguchi, Y.; Okada, T.; Kido, G.; Wakasa, M. *Chem. Lett.* **2005**, *34*, 1692.
- (15) Hamasaki, A.; Sakaguchi, Y.; Nishizawa, K.; Kido, G.; Wakasa, M. *Mol. Phys.* **2006**, *104*, 1765.
- (16) Wakasa, M.; Hayashi, H. *J. Phys. Chem.* **1996**, *100*, 15640.
- (17) Sakaguchi, Y.; Hayashi, H.; Nagakura, S. *J. Phys. Chem.* **1982**, *86*, 3177.
- (18) Wakasa, M.; Nishizawa, K.; Abe, H.; Kido, G.; Hayashi, H. *J. Am. Chem. Soc.* **1999**, *121*, 9191.
- (19) Feed, J. H. *Chemically Induced Magnetic Polarization*; Muus, L., Atkins, P. W., McLauchlan, K. A., Pedersen, J. B., Eds.; D. Reidel: Dordrecht, The Netherlands, 1977; Chapter 19.
- (20) Pedersen, J. B. *J. Chem. Phys.* **1977**, *67*, 4097.
- (21) Hamaguchi, H.; Ozawa, R. *Adv. Chem. Phys.* **2005**, *131*, 85.
- (22) Wang, Y.; Voth, G. A. *J. Phys. Chem. B* **2006**, *110*, 18601.
- (23) Nishikawa, K.; Wang, S.; Katayanagi, H.; Hayashi, S.; Hamaguchi, H.; Koga, Y.; Tozaki, K. *J. Phys. Chem. B* **2007**, *111*, 4894.
- (24) Funston, A. F.; Fadeeva, A. F.; Wishart, J. F.; Castner, E. W., Jr. *J. Phys. Chem. B* **2007**, *111*, 4963.
- (25) Hayashi, H.; Nagakura, S. *Bull. Chem. Soc. Jpn.* **1984**, *57*, 322.
- (26) Nakamura, Y.; Igarashi, M.; Sakaguchi, Y.; Hayashi, H. *Chem. Phys. Lett.* **1994**, *217*, 387.
- (27) Nishizawa, K.; Sakaguchi, Y.; Abe, H.; Kido, G.; Hayashi, H. *Mol. Phys.* **2002**, *100*, 1137.
- (28) Wakasa, M.; Hayashi, H.; Mikami, Y.; Takada, T. *J. Phys. Chem.* **1995**, *99*, 13181.